ELSEVIER

Energy and Buildings 28 (1998) 229–235

ENERGY AND BUILDINGS

Study of convective phenomena inside cavities coupled with heat and mass transfers through porous media—application to vertical hollow bricks—a first approach

C. Vasile *, S. Lorente, B. Perrin [1]

Laboratoire d'Etudes Thermiques et Mécaniques, INSA-UPS, INSA Département Génie Civil, Avenue de Rangueil, 31077 Toulouse, France

Abstract

Building structures often contain cavities or strips of air. Because of this, it is difficult to describe the transfer phenomena that are in fact heat transfers (conductive, convective and radiative), as well as mass transfers through porous media. Numerous studies have dealt with each of these transfers separately but few have managed to describe the interrelation between them. This paper represents an initial approach to the problem, by attempting to describe the influence of the moisture level on heat transfers occurring through hollow vertical terra-cotta bricks. A theoretical modeling of exchanges has been carried out in order to determine radiative and convective exchanges coefficients. A mass exchange coefficient has then been deduced. The results obtained show a high sensitivity of the heat flux to the moisture level of the surroundings.

Keywords: Convective phenomena; Mass transfer; Heat transfer

1. Introduction

The purpose of this paper is to contribute to the description of the transfer phenomena within the outer shell of buildings. In order to do this, it is necessary to consider combined heat, air and mass transfers throughout the wall's components. As the envelope contains cavities that can be more or less large, the problem becomes more complex because the heat and mass (vapour) transfers are dependent on thermal convective movements of air. An accurate description of all transfers throughout the wall would imply an accurate description of air movements. The physical models used generally describe the transport phenomena through the parts composed of porous media, but the description of the transport in the cavity is oversimplified. Convection is not adequately described, because macroscopical equivalent properties of air are used. Our project is the first to link the transport phenomena through the porous material and thermal convective movements of air in the cavity. This implies the use of simultaneously numerical codes concerning the solid part and the cavity.

In this paper, the hygrothermal behaviour of vertical hollow bricks is described. Our two dimensional code calculates the transport through the solid part and utilizes two global exchange coefficients for the cavity, one for heat transfer and one for mass transfer. These coefficients can also be considered as global transport properties, but the values used are based on a detailed description of the thermal convective movement of air in the cavity.

In the first part of this paper, the thermal convective exchanges inside a cavity are studied. A mean convective exchange coefficient and a mean mass exchange coefficient are then deduced.

In the second part, the hygrothermal behaviour of hollow bricks in relation to the relative humidity of surroundings is studied and numerical results are presented.

2. Thermal convective exchanges inside cavities

This research stems from a number of results obtained in laboratory tests [1,2], the aim of which were to describe thermal phenomena occurring inside vertical hollow bricks. An experimental study was initially carried out, followed by an attempt to justify theoretically an air strip thermal equivalent resistance, the parameters of which are essential to the discovery of thermal exchange coefficients on the cavity surfaces.

* Corresponding author.

[1] Tel.: +33 561 556709; fax: +33 561 559900; e-mail: perrin@insa-tlse.fr

0378-7788/98/$ - see front matter
PII S0378-7788(97)00058-3

2.1. Experimental studies

2.1.1. Experimental procedures

Fig. 1 represents a single cavity; one active side is maintained at a uniformly warm temperature, the other at uniformly cold temperature. The four other sides are considered as conductive. In Fig. 2, a cross-section of the enclosure shows how are temperatures were measured. Sixteen thermocouple probes (K type, 0.1 mm diameter) were fixed on a small bar fastened to a vertical rod whose displacement is controlled. The cavity was then inserted into an experimental test apparatus usually used to determine the thermal conductivity of materials.

Sources of errors in temperature measurements have been reduced by using thermocouples of 0.3 K accuracy. Moreover, the horizontal position of the probes inside the cavity was determined once the thermocouples were inside. Parallelism between the vertical rod and the cavity faces was checked to ensure correct positioning of the probes.

2.1.2. Different types of measurements

The test apparatus thus set up has enabled us to plot the temperature field in a median surface ($y=L_y/2$) at different values of the Rayleigh number framing the various configurations relating to buildings, stressing the temperature profiles of boundary limits (cf. Fig. 3).

Furthermore, particular attention has been paid to the vertical temperature stratification on the cavity core ($x=L_x/2$, $y=L_y/2$). Three distinct areas can be observed: a central zone taking up two-thirds of the enclosure and two others that demonstrate the influence of the horizontal sides. About 20 different measurements, characterised by various boundary conditions on the temperature and aspect ratio have enabled us to calculate the dimensionless vertical temperature distribution in the core cavity (cf. Fig. 4).

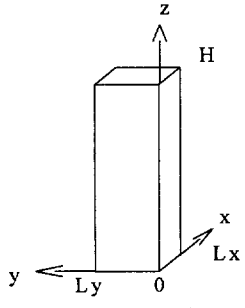

Fig. 1. Single cavity.

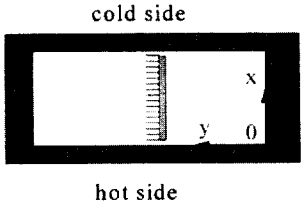

Fig. 2. Cross-section of the cavity and probes.

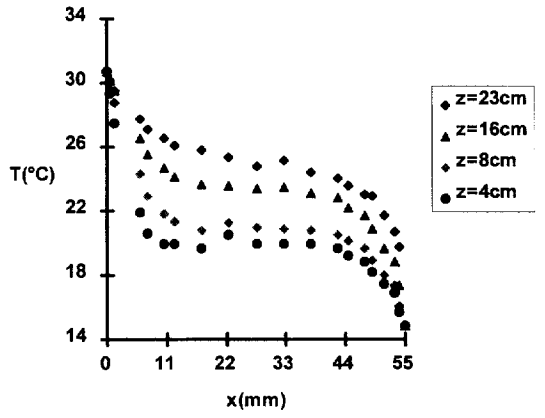

Fig. 3. Temperature profiles on a median surface.

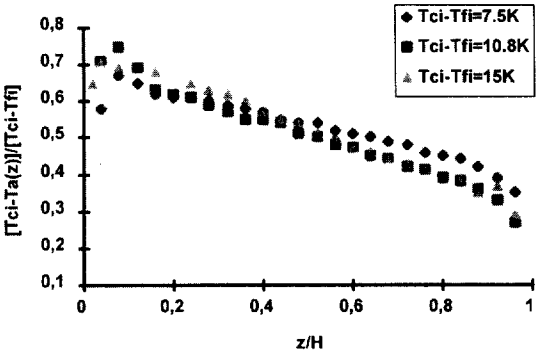

Fig. 4. Stratification.

Before opting for a two-dimensional algorithm to describe thermal transfers, the influence of the restricted vertical sides has been ensured as the example in Fig. 5 shows.

2.2. Theoretical analysis

From the results previously presented, en attempt has been made to find a theoretical justification for the calculation of air strip thermal resistance.

2.2.1. Convective heat transfers

Adapting Karman Polhausen's semi-integral method to the case of cavities, boundary limit equations on an enclosure can be written as:

$$\frac{\partial u}{\partial x}+\frac{\partial w}{\partial z}=0 \tag{1}$$

$$u\frac{\partial w}{\partial x}+w\frac{\partial w}{\partial z}=g\beta(T-Ta(z))+\upsilon\frac{\partial^2 w}{\partial x^2} \tag{2}$$

$$u\frac{\partial T}{\partial x}+w\frac{\partial T}{\partial z}=a\frac{\partial^2 T}{\partial x^2} \tag{3}$$

From temperature and velocity boundary conditions written at the sides and in boundary layers, and using the simplifying hypothesis for air which enables thermal boundary layer thickness to be equivalent to those of velocity the profiles can be written thus:

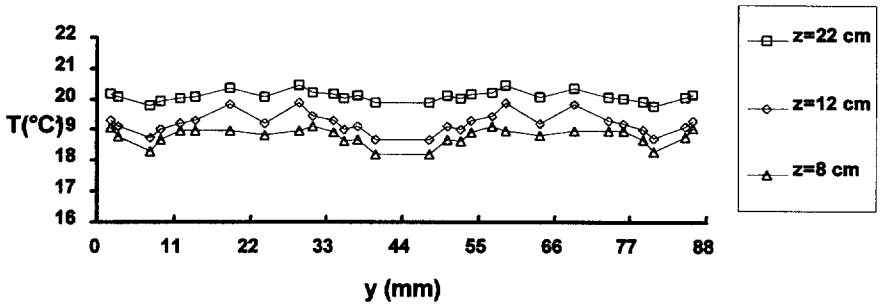

Fig. 5. 2-D flow.

$$\frac{T-Ta(z)}{T_P-Ta(z)}=1-2\theta+2\theta^3-\theta^4 \quad (4)$$

$$\frac{w}{W_{r_f}}=\frac{g\beta\delta^2(z)}{6\upsilon W_{r_f}}(T_P-Ta(z))(1-\theta^3)\theta \quad (5)$$

with:

$$\theta=\frac{x}{\delta(z)} \text{ and } W_{r_f}=g\beta\Delta T_i L_x \quad (6)$$

Resolving the momentum equation in its integral form, the equation

$$\frac{\partial\delta}{\partial z}=\frac{2D}{75\delta^3\tau}-\frac{2\delta}{5\tau}\frac{\partial\tau}{\partial z} \quad (7)$$

has been obtained, where δ was calculated using Runge–Kutta's algorithm.

Local values of heat density are obtained by

$$\frac{\partial\delta}{\partial z}=\frac{2D}{75\delta^3\tau}-\frac{2\delta}{5\tau}\frac{\partial\tau}{\partial z}$$

These local results are then integrated onto the whole cavity to obtain the average convective transfer value.

2.2.2. *Radiative heat transfers*

Heat flux radiated by cavity faces is determined by using radiosity method:

$$\sum_{j=1}^{6}\left[\frac{\delta_{kj}}{\epsilon_j}-F_{kj}\frac{1-\epsilon_j}{\epsilon_j}\right]\frac{Q_j}{S_j}=\sum_{j=1}^{6}(\delta_{kj}-F_{kj})\sigma T_j^4 \quad (8)$$

with: δ_{kj} Kronecker's symbol; ε emissivity; F_{kj} configuration factor; Q_j radiative heat flux; S_j surface; SB Stefan–Boltzmann's constant; T_j temperature.

Once this flux is calculated, an equivalent radiative exchange coefficient can be obtained.

2.2.3. *Thermal resistance of the air strip*

Concluding that overall heat transfer through the cavity is due both to convective and radiative transfers, we can then deduce the value of the equivalent thermal resistance by:

$$R_{th}=\frac{T_{ci}-T_{fi}}{F_{cv}+F_r}$$

In Fig. 6, the thermal resistance variation according to the temperature difference imposed. is shown. A high sensitivity to the variations in boundary conditions can be noted.

On the basis of these results, a value for the exchange coefficients near the sides, can be furnished by integrating convective and radiative phenomena. Thus, we write:

$$h\cong\frac{2}{R_{eq}}$$

This expression implies therefore that thermal heat resistance is only imputable to the effects of the sides, which is well borne out by our experiments.

3. Transfers through porous media

The essential elements of the physical pattern permitting a macroscopic description of the transfers through porous media can now be shown [3–10]. The description is based on a classic process that considers porous media to be continuous. An elementary volume is defined as being is large enough compared with pore dimensions but small enough in relation to the size of the test piece. The parameters (temperature, phase concentrations, etc.) defined on this volume represent average microscopic values. Inside the material, phases are air, vapour and liquid water. The physical problem can be described by the mass and energy conservation equations of the various constituents and the phenomenological laws. Mass conservation water:

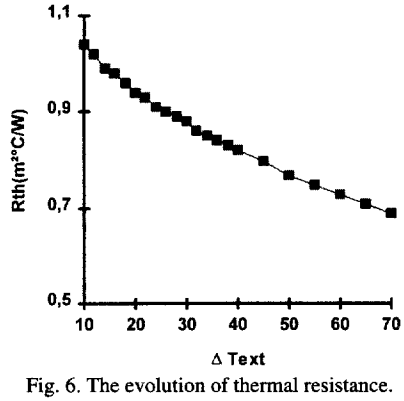

Fig. 6. The evolution of thermal resistance.

$$\frac{\partial}{\partial t}(\rho_s w_l)+\nabla \dot{m}_l = r_l \tag{9}$$

vapour:

$$\frac{\partial}{\partial t}(\rho_s w_v)+\nabla \dot{m}_v = r_v \tag{10}$$

air:

$$\frac{\partial}{\partial t}(\rho_s w_a)+\nabla \dot{m}_a = r_a \tag{11}$$

Energy conservation

$$\rho_0 c_p \frac{\partial T}{\partial t} = \nabla \cdot \phi - L_v \nabla \cdot \dot{m}_v \tag{12}$$

3.1. Phenomenological laws

These enable all the various flow phenomena to be expressed according to the parameter gradients which are producing them. The different phase filtrations are based on Darcy's law. So, in the case of water:

$$\dot{m}_l = \frac{k_l}{v_l} \cdot (\nabla P_l - \rho_l g) \tag{13}$$

Leaving the effect of gravity to one side, mass flux densities of the two gaseous phase components, air and vapour, are:

$$\dot{m}_v = -\omega_v \frac{k_g}{v_g} \cdot \nabla P_g + j_v \tag{14}$$

$$\dot{m}_a = -\omega_a \frac{k_g}{v_g} \cdot \nabla P_g + j_a \tag{15}$$

Furthermore, diffuse vapour and air flux are determined by Fick's law:

$$j_v = -\rho_g D_v f \cdot \nabla \omega_v = -j_a \tag{16}$$

and heat flux is calculated using Fourier's law

$$\Phi = -\lambda \nabla T \tag{17}$$

3.2. Equations system

The following terms have not been taken into account: (i) pressure gradient of the gaseous phase which is then supposed uniform; and (ii) air mass accumulation.

Then, in the case of a one-dimensional transfer, the equations system becomes:

$$\frac{\partial \omega}{\partial t} = \frac{\partial}{\partial x}\left(D_w \frac{\partial \omega}{\partial x} + D_T \frac{\partial T}{\partial x}\right) \tag{18}$$

$$\rho_0 c_p \frac{\partial T}{\partial t} = -L_v \frac{\partial \dot{m}_v}{\partial x} + \frac{\partial}{\partial x}\left(\lambda \frac{\partial T}{\partial x}\right) \tag{19}$$

with:

$$w = w_v + w_l \tag{20}$$

Eqs. (18) and (19) represent mass and heat transfers equations, respectively; Eq. (19) can be written in a different form:

$$\rho_0 c_p \frac{\partial T}{\partial t} = -L_v \epsilon' \frac{\partial \dot{m}}{\partial x} + \frac{\partial}{\partial x}\left(\lambda \frac{\partial T}{\partial x}\right) \tag{21}$$

in order to replace the vapour mass flux density gradient, which cannot be directly measured, by a term composed of total mass flux density gradient, completed with the phase change rate. Indeed, on the bases of our simplifying hypothesis, vapour mass flux density can be expressed by:

$$\rho_0 c_p \frac{\partial T}{\partial t} = -L_v \epsilon' \frac{\partial \dot{m}}{\partial x} + \frac{\partial}{\partial x}\left(\lambda \frac{\partial T}{\partial x}\right) \tag{22}$$

Thus, Eq. (19) becomes:

$$\dot{m}_v = -\rho_g D_v f \cdot \Delta \omega_v \tag{23}$$

The identification of Eq. (23) to Eq. (21) leads to

$$\frac{\partial T}{\partial t} = \frac{\partial}{\partial x}\left[\frac{L_v D_v \rho_g f}{c_p \rho_0}\left(\frac{\partial \omega_v}{\partial w} \cdot \frac{\partial w}{\partial x} + \frac{\partial \omega_v}{\partial T} \cdot \frac{\partial T}{\partial x}\right)\right] + \frac{1}{c_p \rho_0} \cdot \frac{\partial}{\partial x}\left(\lambda \frac{\partial T}{\partial x}\right) \tag{24}$$

with

$$\epsilon' = \frac{\rho_g}{\rho_0} \cdot \frac{D_v}{D_w} \cdot f \cdot \frac{\partial \omega_v}{\partial w} = \frac{\rho_g}{\rho_0} \cdot \frac{D_v}{D_T} \cdot f \cdot \frac{\partial \omega_v}{\partial T} \tag{25}$$

$$\omega_v = \frac{1}{\rho_g} \cdot \frac{p_{v_s}}{R_v T} \varphi \tag{26}$$

We then obtain

$$\epsilon' = \frac{f}{\rho_0} \cdot \frac{D_v}{D_w} \cdot \frac{p_{v_s}}{R_v T} \cdot \frac{\delta \varphi}{\delta w} \tag{27}$$

3.3. Boundary conditions

When a porous media is in contact with a moist air flow at a certain temperature, the material exchanges energy and moisture. A full analysis of this exchange process entails an accurate description of air flow at the brick surface and, particularly, the way in which dynamic, thermal and hydrical boundary layers develop.

As these boundary layers present the same shape, the average mass and heat exchange coefficients, respectively h_m and h_c, defined by:

$$m = \dot{h}_m \Delta \rho_v = h_m (\rho_{v_s} - \rho_{v_a}) \tag{28}$$

$$\varphi = h_e \Delta T = h_c (T_s - T_a) \tag{29}$$

are linked by the relation:

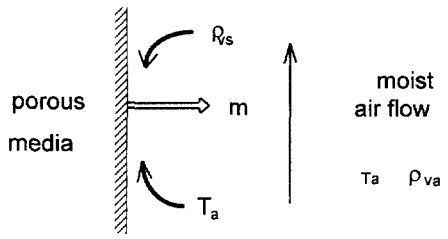

Fig. 7. Exchanges between a porous media and a moist flow.

$$h_m \cong \frac{h_c}{\rho_g c_g} \quad (30)$$

The continuity of temperatures and flux at the boundary of material (Fig. 7), has then to be admitted. Furthermore, porous media are in a state of hydrical balance with the air layer with which it is in contact.

Consequently, in the case of a hollow brick, when the convective part of the global exchange coefficient is known, the mass flux exchanged between moist air and the porous media that constitutes the terra-cotta side can be expressed.

4. The numerical code HYGRO[2]

The two-dimensional numerical code HYGRO described here is an essential element in our study. The results previously indicated concerning convective transfers inside cavities stress the two dimensional nature of exchanges. Therefore, a 2-D approach is justified. The implementation of this code is possible on a PC with at least a 640 KO memory and takes up about 15 MO on a high disk. The grid is composed of 550 nodes, and nine different materials can be taken into account. The discretization is carried out using a non-regular rectangular grid. Around each node, the hygrothermal balance of a rectangular element is considered. In the case where several materials are in contact, there is a discontinuity of water content. On the other hand, materials are there in suction balance. Moreover, four different materials can be considered around a node.

In order to describe exchanges through materials, the equations system linking heat and mass transfer is solved with a finite differences method. All the parameters subjected to experimental determination depend on water content and temperature. Concerning boundary conditions at material/air contact, a hydrical and thermal balance is considered to exist between the material and the boundary layer. Thus, heat flux by the wall is calculated in the air by means of convective and mass exchange coefficients that are linked in accordance with relation (30).

An overall heat and moisture balance is obtained inside the whole cavity in order to calculate the development according to time of temperature and moisture considered as uniform inside the whole cavity volume. Finally, the code provides data about temperature and moisture concentration fields observable in space and time.

[2] HYGRO code was settled by CEBTP in St Rémy les Cheuvreuses.

5. Hygrothermal behaviour of a vertical hollow terra-cotta brick

5.1. Presentation of the studied cases

The previous results as a whole have been calculated in order to describe the behaviour of terra-cotta cavities at various temperature and moisture levels.

Using hollow vertical bricks, 25 cm high, with air thickness of 5.5 cm and width of 8.8 cm, which come very close to the geometric characteristics of building materials, we first focused on an elementary cavity subjected to three temperature differences: 20, 15 and 5°, followed by a two-hollowed brick (Fig. 8). Theses cases correspond to an inner temperature of 20°C and outer temperatures of 0°C, 5°C and 15°C. Heat flux through our bricks, was computed for three vapour pressure differences (Table 1).

As a result of the thermal convective calculations (as presented in Section 2), carried out for each of the above cases, it is possible to determine convective and global exchange coefficients inside cavities as well as heat flux density through the brick. The results of this first initial study are presented

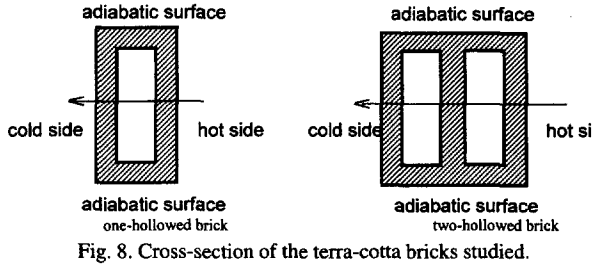

Fig. 8. Cross-section of the terra-cotta bricks studied.

Table 1
Moisture boundary conditions

	Cold surrounding relative moisture Ψ	Hot surrounding relative moisture Ψ
Case 1	50%	50%
Case 2	50%	100%
Case 3	100%	100%

Table 2
One-hollowed brick

One-hollowed brick	a	b	c
Cold surface temperature (°C)	0	5	15
Warm surface temperature (°C)	20	20	20
Convective exchange coefficient: h_c (W/m^2 K)	3.39	2.6	2
Global exchange coefficient: $h=h_c+h_r$ (W/m^2 K)	10.57	9.5	8.7
Heat flux density: ϕ (W/m^2)	123.6	83	26.5

Table 3
Two-hollowed brick

Two-hollowed brick	a	b	c
Cold surface temperature (°C)	0	5	15
Warm surface temperature (°C)	20	20	20
Convective exchange coefficient: h_c (W/m^2 K)	3.31	3.04	2.01
Global exchange coefficient: $h=h_c+h_r$ (W/m^2 K)	10.24	10.05	9.19
Heat flux density: ϕ (W/m^2)	64.03	47.53	15.07

in Table 2 (one-hollowed brick) and Table 3 (two-hollowed brick).

The HYGRO code was then used in each case, to compute the hygrothermal behaviour of the vertical hollow bricks.

5.2. Computed results

5.2.1. One-hollowed brick

These results, as presented graphically in Fig. 9, call for some remarks.

It can be noticed that heat flux through a vertical hollow terra-cotta element increases with the vapour pressure difference. The more the temperature rises, the greater is the increase. These results stress the high heat flux sensitivity to the material moisture concentration level, as differences between a low water content state and one with a more concentrated level are about 35%.

It can be seen further that heat flux calculated from the thermal convective code (Table 2) without taking into account moisture transfers, is very close to that obtained using HYGRO in case b. Indeed, it is here the average water contents are found to be close together insofar as terra-cotta thermal conductivity is 1.2 W/m °C which corresponds to a non-zero water content.

5.2.2. Two-hollowed brick

Here also, the heat flux is notably affected by the moisture level inside the hollow brick However sensitivity seems to be lower in this case than that found previously as the flux increase between the driest case and the most moist case is 25% vs. 35% for a one-hollowed brick.

Furthermore, brick cavities act as a brake on heat and moisture transfer phenomena, and an increase in the number of cavities equally restricts temperature, as well as moisture effects.

6. Conclusion

We have tried in this work to focus on the problem of combined heat and moisture transfer phenomena inside the air cavities and the porous media of brick surfaces. In the case of hollow vertical terra-cotta bricks, the level of influence of moisture on heat transfers has been demonstrated.

Our results are based on the use of a 2-D numerical software, HYGRO, which requires a detailed analysis of the global and convective coefficients inside each cavity, and the hygrothermal behaviour of terra-cotta.

A previous experimental study on thermal convective phenomena inside this type of air pocket indicated that a two-dimensional approach was well justified in order to take into account the kind of air flow and the slight effect of side surfaces.

A numerical method was computed in order to determine exchanges through the bricks; thus, enabling us to calculate an equivalent thermal resistance of the air strip including convective and radiative exchange coefficients. The mass exchange coefficient was then determined using the convective coefficient.

These initial calculations show a high sensitivity of heat flux through hollow bricks according to the moisture level of the surroundings and in consequence the materials, as these flux values can vary from 25% to 35% from low to high humidity.

This paper constitutes an initial approach to the study of combined phenomena occurring during transfers through cavities or air strips and porous media. A complete physical analysis will then be necessary in order to take into account

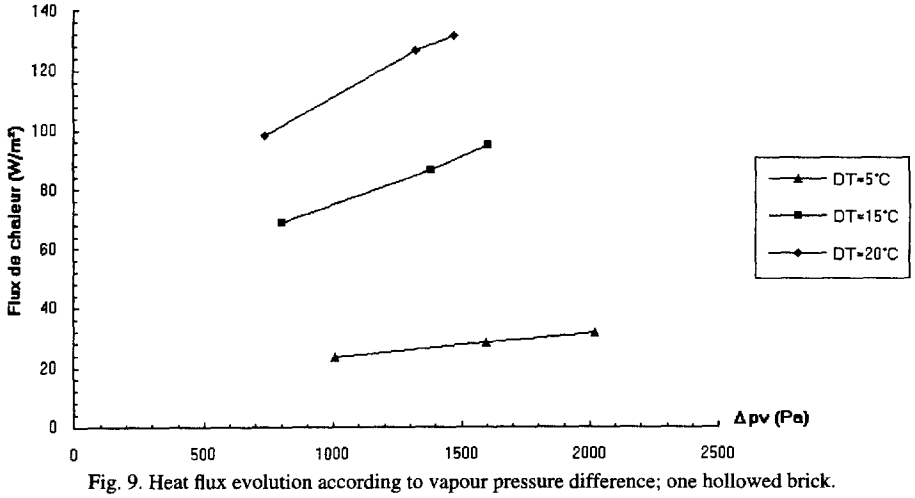

Fig. 9. Heat flux evolution according to vapour pressure difference; one hollowed brick.

more complex situations, for instance, when the air strips are ventilated or when condensation occurs in the cavities.

7. Nomenclature

D_w	Diffusion coefficient	m^{-2} s
H	Height	m
h	Exchange coefficient inside cavity	W m^{-2} K^{-1}
h_c	Convective exchange coefficient	W m^{-2} K^{-1}
h_r	Radiative exchange coefficient	W m^{-2} K^{-1}
h_m	Mass exchange coefficient	m s^{-1}
Ψ	Relative moisture of surroundings	%
j_a	Diffusive air flux	kg m^{-1} s^{-1}
j_v	Diffusive vapour flux	kg m^{-1} s^{-1}
L_v	Water vaporization energy	J kg^{-1}
L_x	Cavity thickness (Ox axis)	m
L_y	cavity thickness (Oy axis)	m
m	Moisture flux	kg m^{-2} s
p_a	vapour pressure	Pa
p_{vs}	saturated vapour pressure	Pa
T	Absolute temperature	K
$Ta(z)$	Temperature in the cavity core ($x=L_x/2$; $y=L_y/2$)	°C
T_{HI}	Internal surface temperature of the cavity active face—warm side	°C
T_{CI}	Internal surface temperature of the active cavity surface—cold side	°C
T_P	Internal surface temperature of the active cavity surface	°C
w	Water content	g kg^{-1}

Greek letters

δ	Boundary layer thickness	m
δw	Difference in water contents	g kg^{-1}
ε'	Changing phase rate	
ϕ	Heat flux density	W m^{-2}
Φ	Heat flux	W
$\phi_{conv}(z)$	Local convective heat flux density	W m^{-2}
λ	Thermal conductivity	W m^{-1} K^{-1}
ρ_0	Volumetric mass of the dry material	kg m^{-3}

Subscripts

a	Air
g	Gazeous phase
l	Water
v	Vapour

References

[1] S. Lorente, Contribution à l'étude des transferts thermiques dans les alvéoles verticales, Application aux produits de terre cuite, Modélisation et expérimentation, Thèse de doctorat, INSA, Toulouse, 1996.

[2] S. Lorente, M. Petit, R. Javelas, Simplified analytic model for thermal transfer in vertical hollow brick, Energy and Buildings, Vol. ENBO 24/2, 1996, pp. 95–103.

[3] Heat, Air and Moisture Transfer in Insulated Envelop Parts, International Energy Agency, Energy conservation in Buildings and Community Systems Programme, Final Report, 24th Annex, 1996.

[4] B. Perrin, Etude des transferts couplés de chaleur et de masse dans des matériaux poreux consolidés non saturés utilisés en Génie Civil, Thèse d'Etat, Université Paul Sabatier, Toulouse, 1985.

[5] B. Dwi Argo, Détermination expérimentale de l'influence de l'hystérésis sur les propriétés hydriques de matériaux poreux du Génie Civil, Thèse de doctorat, INSA, Toulouse, 1994.

[6] P. Crausse, J.P. Laurent, B. Perrin, Influence des phénomènes d'hystérésis sur les propriétés hydriques de matériaux poreux. Comparaison des modèles de simulation de comportement hydrique, Revue Générale de Thermique, Vol. 35, No. 35, February 1996.

[7] D.A. De-vries, The theory of heat and moisture transfer in porous media revisited. International Journal of heat and mass transfer. Vol. 30 No. 7 July 1987.

[8] M. Quintard, M. Todorovic, Heat and Mass Transfer in Porous Media, Elsevier, 1992.

[9] J. Bear, M. Yaruz Corpacioglu, Fundamentals of transport phenomena in porous media, NATO ASI Series No. 82, 1984.

[10] Drying '92 Proceedings of the 8th, International Drying Symposium (IDS '92), Montreal, August 1992.